



Contents lists available at ScienceDirect

Chinese Chemical Letters

journal homepage: www.elsevier.com/locate/cclet



Communication

Exploring the *N*-terminus region: Synthesis, bioactivity and 3D-QSAR of allatostatin analogs as novel insect growth regulators

Meizi Wang, Li Zhang, Xianwei Wang, Yun Ling, Xiaoqing Wu, Xinlu Li, Yiduo Mi, Xinling Yang*

Department of Applied Chemistry, College of Science, China Agricultural University, Beijing 100193, China

ARTICLE INFO

Article history:

Received 25 September 2017
Received in revised form 13 November 2017
Accepted 16 November 2017
Available online xxx

Keywords:

Allatostatins
Juvenile hormone
IGRs
AST analogs
Synthesis
3D-QSAR

ABSTRACT

Allatostatins (ASTs), a family of insect neuropeptide, can inhibit juvenile hormone (JH) biosynthesis by the corpora allata (CA) in *Diploptera punctata*, and therefore be regarded as potential leads for the discovery of new insect growth regulators (IGRs). But several shortcomings, such as their sensitivity to peptidases and high cost, impeded their practical application in pest management. In order to discover new IGRs, one AST analog **B1** possessing non-peptide group was discovered with high ability to inhibit JH biosynthesis *in vitro* (IC₅₀: 0.09 μmol/L) in our previous studies. In the present work, two series of **B1** analogs with different substituents on the *N*-terminus region were designed and synthesized. The result suggested that benzene showed better activity than other heterocycles, and the *para*-substitution on the benzene was beneficial for activity. Moreover, analogs with log*P* value over 2.0 exhibited good activity, which indicated that the hydrophobicity is important to the bioactivity. Three dimension quantitative structure-activity relationship (3D-QSAR) studies were performed to highlight the structural requirements of AST analogs, which demonstrated introduction of bulkier substituents on the *N*-terminus would increase the activity. Analog **II12** (IC₅₀: 0.08 μmol/L) exhibited similar inhibitory activity to the lead **B1**, but its synthetic route was simpler than **B1**. Therefore, **II12** could be used as a new lead compound for the discovery eco-friendly IGRs.

© 2017 Chinese Chemical Society and Institute of Materia Medica, Chinese Academy of Medical Sciences.
Published by Elsevier B.V. All rights reserved.

Thanks to the virtue of high potency, good selectivity and eco-friendly safety, insect growth regulators (IGRs) are regarded as the ideal pesticides in the 21st century [1]. The discovery of new IGRs has therefore become increasingly important in pest control both in agriculture and public health. The FGLamide allatostatins (FGLA-ASTs), originally isolated from the cockroach *Diploptera punctata* in 1989, have 6–18 amino acids and inhibit juvenile hormone (JH) biosynthesis by the corpora allata [2]. Allatostatins (ASTs) also exhibited pleiotropic functions including modulation of myotropic activity in both gut and dorsal vessel [3], inhibition of vitellogenin production in the fat body [4], stimulation of carbohydrate enzyme activity in the midgut [5]. With these abilities to influence a number of physiological processes, especially inhibition of JH biosynthesis in some insect species, ASTs were regarded to be potential leads for the discovery of new IGRs.

However, some shortcomings, such as their susceptibility to both exo- and endopeptidases in hemolymph and tissues of insects

and high production cost, preclude their application in pest management [6]. To find analogs that overcome these limitations while retain activity, structural modifications and structure-activity relationships (SARs) have been carried out in recent years. There are several susceptible hydrolysis sites in the core pentapeptide of the FGLA-ASTs which shared a common conserved C-terminal sequence Y/FXFGL-NH₂ (X = A, N, G, and S) for activity [7]. The primary site is between Y/F and X residue, which was susceptible to cleavage by the enzymes of hemolymph [8,9]. Replacing the specific amino acids with non-amino acid, Nachman had synthesized some ASTs analogs which retained the ability of inhibition JH biosynthesis and displayed resistance to degradation [6]. Kai replaced Y with a non-peptide structure (aromatic group) and obtained some analogs with enhanced resistance to peptidase hydrolysis [10]. Using the peptidomimetics strategy, Xie found a new simple mimic **B1** for T/YXFG, with higher activity than the lead core pentapeptide [11]. Previous study demonstrated that these positions tolerated a range of non-amino acid replacement.

Introduction non-amino acid groups can not only protect peptidase-susceptible sites but also reduce the production cost. With the purpose to study the substituents effects of the *N*-

* Corresponding author.

E-mail address: yangxl@cau.edu.cn (X. Yang).

<https://doi.org/10.1016/j.ccl.2017.11.022>

1001-8417/© 2017 Chinese Chemical Society and Institute of Materia Medica, Chinese Academy of Medical Sciences. Published by Elsevier B.V. All rights reserved.

terminus region on JH inhibitory activity and to explore the structure-activity relationship as well as to highlight the structural requirements of AST analogs for further discovering new analogs with higher activity and simpler structure, we designed two series of ASTs analogs by modifying the *N*-terminus region of lead **B1** via replacing 1*H*-benzotriazole with aniline, heterocyclic amines or other substitutes (the design strategy is shown in Fig. 1). The target compounds were prepared via a simpler synthetic route in the present work and their structures were confirmed by ¹H NMR, ¹³C NMR and HRMS. Their inhibition of JH biosynthesis against *Diploptera punctata* was evaluated *in vitro* and the preliminary structure-activity relationship was analyzed. In addition, 3D-QSAR studies were performed to explore the vital factors for designing new IGRs candidate.

The synthesis of analog **B1** (1) and analog **II12** (2) was illustrated in Scheme S1 (Supporting information). The rest analogs were obtained using the same synthetic route (2). Leu with resin was synthesized from Rink amide-AM resin (1 equiv.) using the standard Fmoc/tBu chemistry and HBTU/HOBt protocol [12,13]. Fmoc-Leu-OH (3 equiv.) was activated with HBTU (3 equiv.), HOBt (3 equiv.) and DIEA (6 equiv.) in DMF for 5 min, and couplings were run for 4 h. Removal of the *N*-terminus Fmoc group from the residues was accomplished with 20% piperidine in DMF for 20 min. Compound **2** was obtained from compound **1** (8 equiv.) which was coupled to the Leu with resin with Dic (4 equiv.) in DMF for 4 h at room temperature [14]. The product with the resin was prepared by the acyl reaction of compound **2** with 4-aminobenzotrifluoride in DMF for 8 h, and then the product was cleaved from the resin with TFA containing 5% water for 2.5 h at room temperature. The crude compounds were purified on a C18 reversed-phase preparation column with a flow rate of 10 mL/min using acetonitrile/water (50:50) at room temperature. UV detection was at 215 nm. The physical and identification data (melting point, ¹H NMR and HRMS of all target compounds and ¹³C NMR of typical analogs **I2** and **II12**) are given in the Supporting information.

The method involves the acyl reaction and solid phase peptide synthesis. Using the reported method [11], the lead **B1** was obtained totally in nine steps and twice purification. The key intermediate compound **2** was cleaved with TFA and then the solution was purified on a C18 reversed-phase preparative column and freeze-dried *in vacuo*. The crude target compound **B1** was obtained by repeating above purification steps. In the present work with purpose to simplify the route and reduce the cost, the

compound **2** was directly reacted with 4-aminobenzotrifluoride followed by cleavage and purification, and we successfully obtained the target compound **II12**. Comparing to lead **B1**, the route of **II12** was shortened from nine steps with twice purification to eight steps with once purification. Moreover, the dosage of HPLC grade solvent used in target compounds preparation was reduced by half.

Natural ASTs are susceptible to inactivation *in vivo* as a consequence of hydrolysis by hemolymph and poor penetration through the insects. The primarily hydrolytic site of the core pentapeptide between the residues Y/F-X and the other hydrolytic site such as G-L was also detected [6]. Analog with modification and replacement of amino acids at the hydrolysis not only showed resistance to peptidases but also retained their bioactivities. In our previous study [11], analog **B1**, a new mimic for Y/FXFGI in which Y was replaced with 4-(1*H*-benzo[d][1,2,3]triazol-1-yl)-4-oxobutanoic acid, showed good inhibition activity without hydrolytic site. To find new analogs with higher bioactivity and lower cost, further optimization on **B1** was carried out in present work. As shown in Fig. 1, the first step of the strategy was to replace the *N*-terminus 1*H*-benzotriazole with aniline and heterocyclic amines (Series I). The bioassay result indicated that analog **I1** with *N*-terminus containing benzene showed the best activity. We subsequently selected **I1** as the second lead, and a series of analogs (Series II) with different substituents on benzene at the *N*-terminus were designed and synthesized to explore the substituent effect on the benzene ring.

According to the results shown in Table 1, most of the target analogs showed obvious ability to inhibit JH biosynthesis by the corpora allata (CA) of *D. punctata* *in vitro* at 1×10^{-5} mol/L. Analog showing inhibition rate more than 70% were chosen to determine their IC₅₀ values. The results indicated that these analogs had different potencies owing to vary modification at *N*-terminus. Series I (**I1–I5**), in which aniline and heterocyclic amines mimicked the 1*H*-benzotriazole region, showed lower activity than **B1**. However, analog **I1** showed the best activity compared to other analogs of series I and therefore was chosen to be the second lead for further optimization. Fortunately, we found that the activities of series II were higher than that of series I. Fig. 2 clearly exhibited that different positions of substituents on the benzene ring at *N*-terminus can lead to different activities. In particular, substituents in the phenyl *para*-position were beneficial for activity compared with *meta*- and *ortho*- substituents (*p*-F (**II6**) > *m*-F (**II5**) > *o*-F (**II4**)). Meanwhile, in the same *para*-position on the phenyl ring, the

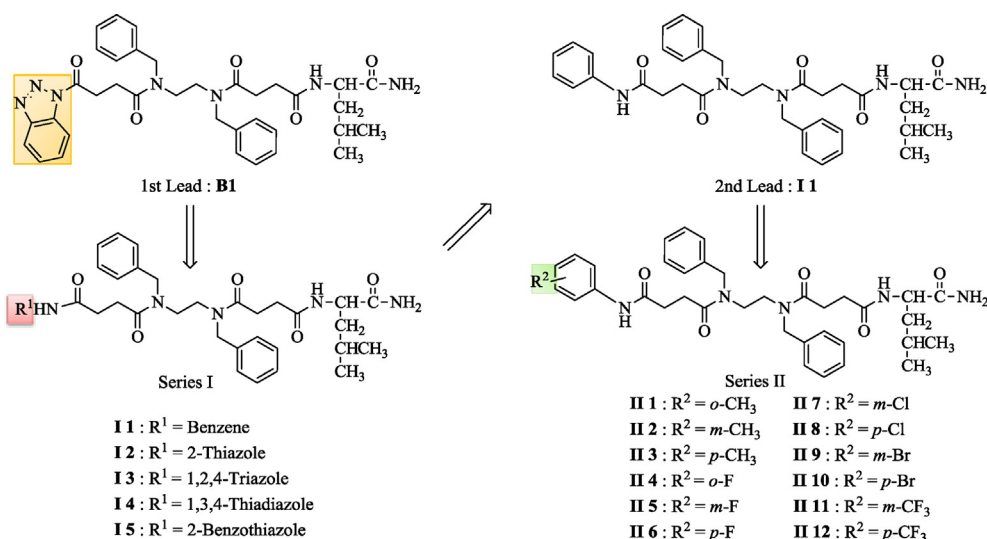
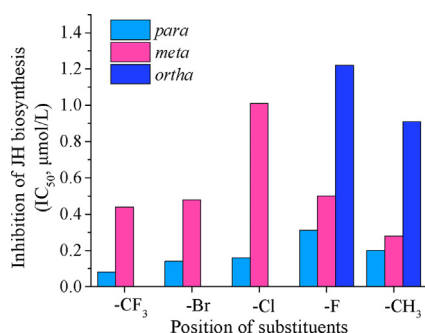


Fig. 1. Design strategy of the *N*-terminus modified **B1** analogs.

Table 1
Activity and log*P* of AST analogs.

Compd.	Inhibition rate (%)	IC ₅₀ (μmol/L)	Log <i>P</i>
B1	87.30	0.09	2.23
I1	87.82	2.29	3.11
I2	81.08	3.93	2.54
I3	73.96	^a	1.90
I4	81.31	2.99	3.76
I5	70.13	^a	0.76
II1	77.85	0.91	3.22
II2	82.07	0.28	3.62
II3	80.07	0.20	3.59
II4	88.63	1.22	3.22
II5	88.39	0.50	3.45
II6	83.14	0.31	3.35
II7	88.57	1.01	4.01
II8	91.63	0.16	3.87
II9	87.14	0.48	4.08
II10	87.44	0.14	4.15
II11	89.29	0.44	4.12
II12	89.69	0.08	4.09

^a IC₅₀ value was much higher than 1 μmol/L, and it could be defined as less active.

**Fig. 2.** Effect of different position of substituent at benzene ring on inhibition of JH biosynthesis. IC₅₀ values determined from dose-response curves whose data points represent means of more than eight replicates.

electron-withdrawing substituents contributed to better activity than that of electron-donating groups, such as (*p*-CF₃ (**II12**) > *p*-Br (**II10**) > *p*-Cl (**II8**) > *p*-CH₃ (**I3**)). However, compound **II6** with *p*-F was an exception due to the following reasons: (1) The activity might be also associated with its steric effect and the radius of fluorine atoms is smaller than methyl group; (2) The hydrophobicity capacity may be benefit for its activity and the lipophilicity of **II6** was weaker than that of **I3**. Compound **II12** (*p*-CF₃) exhibited the highest activity (IC₅₀: 0.08 μmol/L), which was close to the 1st lead **B1** (IC₅₀: 0.09 μmol/L).

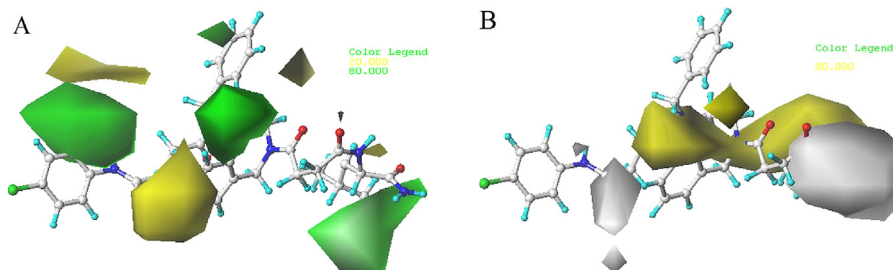
In the previous work [15], it was supposed that the potency of the AST analogs may be related to their lipophilicity. To elucidate the relationship between hydrophobicity and the inhibition activity, the log*P* values of target analogs were calculated by the prediction system (Table 1). The results obviously exhibited that

these AST analogs with log*P* values less than 2.0 exhibited poor activity (**I3**, log*P*=1.9) and (**I5**, log*P*=0.76). Analogues with log*P* more than 2.0 showed visible activity. This indicated that a suitable hydrophobicity may be important to activity. Possibly, these analogs with strong lipophilic capability may easily penetrate the cell membrane and interaction with the *Dippu*-AST receptor, consequently exhibit potent effects. However, the above hypothesis needs more evidences to validate.

The results of CoMFA and CoMSIA model are showed in Table S1 (Supporting information). The predicted *r*² for CoMFA (*r*²_{test}=0.878) was lower than that for CoMSIA (*r*²_{test}=0.891), indicating that CoMSIA had better predictive ability. The scattered plot of the predicted activity data versus the experimental data showed in Fig. S2 (Supporting information) and the values showed in Table S2 (Supporting information). The good correlations prove the robustness and good predictive ability of the optimal CoMSIA model.

Two significant effects map (Fig. 3A (steric) and Fig. 3B (hydrophobic)) were built with CoMSIA method. In the region A (*N*-terminus) of Fig. 3A, the steric contours of the CoMSIA displayed a large green contour, which indicated the favorable effect of bulky groups on increasing the biological activities of molecules. For instance, bulkier groups such as -CH₃ (**II1**–**II3** with pIC₅₀=6.040, 6.545, 6.710) in contrast to -H (**I1** with pIC₅₀=5.640) in region A could increase the biological activities. This is according with above result which the activity of analogue **I3** with *p*-CH₃ was higher than that of **II6** with *p*-F. This was also observed among molecules **I3**–**II12** having F, Cl, Br, CF₃ group respectively. The larger the substituent, the better activity it has. The order of inhibition activities are *p*-CF₃ (**II12**) > *p*-Br (**II10**) > *p*-Cl (**II8**) > *p*-F (**II6**) and *m*-CF₃ (**II11**) > *m*-Br (**II9**) > *m*-Cl (**II7**). From Fig. 3B, two white contours in region C (2 site amino acid at *N*-terminus) and carbon terminus respectively, indicated that introduction of hydrophilic substituents in these regions will benefit for inhibitory activity. That further pIC₅₀ values are needed to illustrate this model.

Two series of novel peptidomimetic analogs were designed and synthesized. The activity of inhibition JH biosynthesis showed that most analogs exhibited considerable activity, especially analogue **II12** (IC₅₀: 0.08 μmol/L) exhibited similar activity to the lead compound **B1** (IC₅₀: 0.09 μmol/L). The preparation procedure was simplified and the production cost was reduced roughly. Primary structure-activity relationship revealed that *para*-substituent had an obvious influence on activity. The proper lipophilicity (log*P* over 2) is favorable for activity. 3D-QSAR models were obtained with high accuracy and predictive ability. The CoMSIA analysis indicated that a significant steric arrangement, where bulkier substituents are aligned on the *N*-terminus region, positively correlates with activity. In addition, introduction of hydrophilic substituents in 2 site amino acid at *N*-terminus will be benefit for inhibitory activity. These results provide useful clues for further chemical modifications and the *in vivo* activity of some promising compounds will be tested in our next optimization work on discovering potential IGRs.

**Fig. 3.** Contour maps of CoMSIA: (A) Steric field and (B) Hydrophobic field.

Acknowledgments

We are very grateful to Professor Stephen S. Tobe for his kind help on bioassay of JH production inhibition *in vitro*. This study was financially supported by the National Natural Science Foundation of China (No. 21372257) and the grants from the National Key Research and Development Plan (No. 2017YFD0200504).

Appendix A. Supplementary data

Supplementary data associated with this article can be found, in the online version, at <https://doi.org/10.1016/j.ccllet.2017.11.022>.

References

- [1] S.M. Olieff, H.J. Mosson, J.P. Edwards, et al., *Int. Pest Control* 39 (1997) 44–45.
- [2] A.P. Woodhead, B. Stay, S.L. Seidel, M.A. Khan, S.S. Tobe, *Proc Natl Acad Sci U.S.A.* 86 (1989) 5997–6001.
- [3] L. Vilaplana, J.L. Maestro, M.D. Piulachs, X. Bellés, J. *Insect Physiol.* 45 (1999) 1057–1064.
- [4] D. Martín, M.D. Piulachs, X. Bellés, *Mol. Cell. Endocrinol.* 121 (1996) 191–196.
- [5] M. Fusé, J.R. Zhang, E. Partridge, et al., *Peptides* 20 (1999) 1285–1293.
- [6] R.J. Nachman, C.S. Garside, S.S. Tobe, *Peptides* 20 (1999) 23–29.
- [7] B. Stay, A.P. Woodhead, S. Joshi, et al., Allatostatins, in: J.J. Menn, T.J. Kelly, E.P. Masler (Eds.), *Insect Neuropeptides*, American Chemical Society, Washington DC, 1991, pp. 164–176.
- [8] A.S. Ripka, D.H. Rich, *Curr. Opin. Chem. Biol.* 2 (1988) 441–452.
- [9] A. Giannis, F. RübSam, Peptidomimetics in drug design, in: B. Testa, U.A. Meyer (Eds.), *Advances in Drug Research*, Academic Press, San Diego, 1997, pp. 1–78.
- [10] Z.P. Kai, Y. Xie, J. Huang, et al., *J. Agric. Food Chem.* 59 (2011) 2478–2485.
- [11] Y. Xie, Z.P. Kai, S.S. Tobe, et al., *Peptides* 32 (2011) 581–586.
- [12] E.G. Brown, J.M. Nuss, *Tetrahedron Lett.* 38 (1997) 8457–8460.
- [13] L.A. Carpino, *Acc. Chem. Res.* 20 (1987) 401–407.
- [14] W.C. Chan, P.D. White, *Fmoc Solid Phase Peptide Synthesis: A Practical Approach*, Oxford University Press, New York, 2000.
- [15] X.Q. Wu, J. Huang, M.Z. Wang, et al., *Chin. Chem. Lett.* 27 (2016) 559–562.